



OPEN ACCESS

EDITED BY

Federico Brucoli,
De Montfort University, United Kingdom

REVIEWED BY

Renee Fleeman,
University of Central Florida, United States
Rahul Saxena,
Georgetown University, United States
Julia Grimwade,
Florida Institute of Technology, United States

*CORRESPONDENCE

Anders Løbner-Olesen
✉ Lobner@bio.ku.dk

RECEIVED 09 February 2024

ACCEPTED 15 March 2024

PUBLISHED 08 April 2024

CITATION

Campion C, Charbon G, Nielsen PE and
Løbner-Olesen A (2024) Targeting synthesis
of the Chromosome Replication Initiator
Protein DnaA by antisense PNA-peptide
conjugates in *Escherichia coli*.
Front. Antibiot. 3:1384390.
doi: 10.3389/frabi.2024.1384390

COPYRIGHT

© 2024 Campion, Charbon, Nielsen and
Løbner-Olesen. This is an open-access article
distributed under the terms of the [Creative
Commons Attribution License \(CC BY\)](#). The
use, distribution or reproduction in other
forums is permitted, provided the original
author(s) and the copyright owner(s) are
credited and that the original publication in
this journal is cited, in accordance with
accepted academic practice. No use,
distribution or reproduction is permitted
which does not comply with these terms.

Targeting synthesis of the Chromosome Replication Initiator Protein DnaA by antisense PNA-peptide conjugates in *Escherichia coli*

Christopher Campion^{1,2}, Godefroid Charbon², Peter E. Nielsen¹
and Anders Løbner-Olesen^{2*}

¹Department of Cellular and Molecular Medicine, University of Copenhagen, Copenhagen, Denmark,

²Department of Biology, University of Copenhagen, Copenhagen, Denmark

Initiation of chromosome replication is an essential stage of the bacterial cell cycle that is controlled by the DnaA protein. With the aim of developing novel antimicrobials, we have targeted the initiation of DNA replication, using antisense peptide nucleic acids (PNAs), directed against DnaA translation. A series of anti-DnaA PNA conjugated to lysine-rich bacterial penetrating peptides (PNA-BPPs) were designed to block DnaA translation. These anti-DnaA PNA-BPPs inhibited growth of wild-type *Escherichia coli* cells at low micromolar concentrations, and cells exposed to anti-DnaA PNA-BPPs exhibited characteristic hallmarks of chromosome replication inhibition. These results present one of very few compounds successfully targeting initiation of chromosome replication, an essential step in the bacterial cell cycle.

KEYWORDS

novel antibiotics, antisense PNA-peptide, chromosome replication, DnaA initiator protein, inhibition of initiation, *Escherichia coli*

Introduction

The burden of increased antibiotic resistance has led to a growing, urgent demand for the discovery and development of novel antibiotic therapeutic strategies. Peptide nucleic acid (PNA) is a potent DNA mimic, with the potential to provide an avenue to antisense drugs combatting bacterial pathogens (Good et al., 2001; Ghosal, 2017; Lee et al., 2019; Saabach et al., 2019; Wojciechowska et al., 2020; Iubatti et al., 2022). In PNA, the sugar backbone of natural nucleotides is replaced by a neutral pseudo-peptide backbone, consisting of 2-amino-ethyl-glycin (aeg) units (Nielsen et al., 1991). PNA forms stable duplexes with sequence complementary DNA and RNA, based on the Watson-Crick hydrogen recognition (Egholm et al., 1993), with higher stability than duplexes formed by

natural phosphodiester backbone nucleic acids. For antimicrobial approaches, PNA is usually designed as 10–12-nucleobases long PNA oligomers to target mRNA transcripts of essential genes. A region between the start codon and the ribosomal binding site is most frequently used as a PNA target site, as this leads to steric hindrance of translation initiation (Good et al., 2001; Dryselius et al., 2003; Goltermann et al., 2019). Unmodified PNA is not readily taken up by bacterial cells (Good and Nielsen, 1998; Good et al., 2000) but must be conjugated to a delivery moiety such as a bacterial-penetrating peptide (BPP) (Good et al., 2001) to translocate across the bacterial envelope. Subsequently, antimicrobial PNA-BPPs against many pathogens using a variety of BPP conjugates and targeting a variety of genes have been described (Ghosal, 2017; Narenji et al., 2017; Lee et al., 2019; Campion et al., 2021).

Replication of the *E. coli* chromosome is initiated from *oriC*, from which the two nascent replication forks proceed bidirectionally, reaching completion at the terminus, *ter* region, after which two fully replicated chromosomes are segregated to daughter cells (for reviews, see Wolanski et al., 2014; Frimodt-Møller et al., 2024). The highly conserved DnaA protein initiates DNA replication by binding to specific “DnaA-boxes” in *oriC*, thereby facilitating strand opening at an AT-rich “DNA unwinding element, DUE” region (Bramhill and Kornberg, 1988), where two replisomes are subsequently assembled (Frimodt-Møller et al., 2024). The *E. coli* DnaA protein contains four domains: an N-terminal protein interaction domain (Domain I); a linker domain (Domain II); an AAA+ ATPase domain, responsible for ATP/ADP binding and ATP hydrolysis (Domain III); and a double-stranded DNA binding domain (Domain IV) (Hansen and Atlung, 2018; Frimodt-Møller et al., 2024).

Only the ATP-bound form of DnaA (DnaA^{ATP}) is active in initiation (Sekimizu et al., 1987) and binds to low-affinity DNA-boxes in *oriC*, forming a structure causing a superhelical tension at the DUE region, which in turn results in DNA strand opening, that is, open complex formation (Erzberger et al., 2006; Ozaki et al., 2008). DnaA subsequently recruits two hexameric DnaB helicase complexes to the DUE region, which eventually leads to the assembly of two replisomes (Sakiyama et al., 2022). (For a thorough review of *oriC* structure and interactions with DnaA and other initiation factors, see Frimodt-Møller et al., 2024). It is essential that the initiation of chromosome replication is tightly controlled in the cell cycle, as the inability to initiate chromosome replication leads to chromosome loss (Botello and Nordstrom, 1998), whereas uncontrolled initiations are detrimental to genome integrity and result in chromosome breaks and cell death (Simmons et al., 2004; Charbon et al., 2014). It is therefore not surprising that the initiation frequency is controlled by a stringent system of mechanisms to ensure that initiation occurs only once per cell cycle, and simultaneously from all cellular origins (Skarstad et al., 1986). For thorough reviews on mechanisms controlling the initiation of DNA replication in *E. coli*, see Katayama et al. (2017), Hansen and Atlung (2018), and Frimodt-Møller et al. (2024).

In the present study, we designed and characterized antisense PNA-BPPs targeting translation of the chromosomal replication initiator protein, DnaA. We show that *E. coli* is sensitive to DnaA-targeting PNA-BPPs in the micromolar range. PNA-BPP target specificity was verified directly by Western blotting and indirectly by a DnaA-inhibitor assay. Cell cycle parameters obtained by flow cytometry and *in vivo* fluorescent microscopy all revealed phenotypic hallmarks of a true inhibitor of chromosomal replication initiation.

Materials and methods

Bacterial growth conditions

Cells were grown at 37°C in non-cation adjusted Mueller-Hinton broth (MHB-I; Sigma Aldrich, Darmstadt, Germany), Lysogeny Broth (LB), or in AB minimal medium (Clark and Maaløe, 1967) supplemented with 10 µg/mL of thiamine, 0.2% glucose or 0.2% glycerol and 0.5% casamino acids. Antibiotics were used at the following concentrations: ampicillin (150 µg/mL), chloramphenicol (20 µg/mL), kanamycin (50 µg/mL), streptomycin (100 µg/mL), tetracycline (10 µg/mL), cephalixin (36 µg/mL), and rifampicin (300 µg/mL).

Bacterial strains

All strains used in this study are listed in [Supplementary Table 1](#). ALO8290 was created by the P1 transduction of *dnaA46* with *tnA:Tn10* into ALO4223 using a P1 lysate of the strain ALO2342 and selecting for tetracycline resistance and screened for thermo-sensitivity.

The R1-based plasmid pJEL-*dnaA*, was constructed by amplifying the *dnaA* gene, including promoter regions (*dnaA1p* and *dnaA2p*) of MG1655 using primers 5'-CCAGAAGCTTAAG CCAATTTTTGTCTATGG-3' and 5'-CCAGGGATCCGTT GTAGCGGTTTTAATAAAA-3'. The PCR product was digested with *HindIII* and *BamHI* and ligated into plasmid pJEL109 (Lobner-Olesen et al., 1992), previously digested with the same enzymes. ALO8528, used for DnaA depletion, was created by deletion of *dnaA* in MG1655 carrying plasmids pJEL-*dnaA* and pKG339 (Jensen et al., 1995) by P1 transduction, using a lysate of the strain TC3478 carrying the Δ *dnaA::cat* mutation (Ingmer and Atlung, 1992).

Antisense PNA design, synthesis, and handling

Antisense PNA were designed as 10-mer nucleobase oligomers, to complement the region between the Shine-Dalgarno sequence and the start codon on the *dnaA* mRNA transcript of the strain MG1655 (NCBI: ref. NC_000913.3) (Table 1). Selected sequences

TABLE 1 PNA-BPP conjugates.

PNA	Sequence including BPP (N-C)	Location to target gene (5'-3')	MIC (μ M)
DnaA-1-PNA	H-(KFF) ₃ K-eg1-TCCACTCGAA-NH ₂	<u>UUCGAGUGGAGUCCGCCGUG</u>	4
DnaA-2-PNA	H-(KFF) ₃ K-eg1-CTCCACTCGA-NH ₂	<u>UUCGAGUGGAGUCCGCCGUG</u>	4
DnaA-3-PNA	H-(KFF) ₃ K-eg1-ACTCCACTCG-NH ₂	<u>UUCGAGUGGAGUCCGCCGUG</u>	2
Mismatch PNA	H-(KFF) ₃ K-eg1-ACC CC ATTCG-NH ₂	Na	16

Complete sequences of anti-DnaA PNA-BPPs along with their binding target on the mRNA. The dnaA start codon is highlighted with bold; the PNA binding position is underlined. PNA-BPPs were synthesized as described (Yavari et al., 2021). Na, not applicable; eg1, 8-amino-3,6-dioxoactanoic acid.

were checked for target specificity to *dnaA* using the NCBI BLASTn software (<https://blast.ncbi.nlm.nih.gov/Blast.cgi>; Supplementary Table 2). PNA-BPPs were synthesized by the continuous standard peptide solid-phase peptide synthesis (SPPS), with tBoc protected monomers, on an MBHA resin. The lysine-rich (KFF)₃K carrier peptide was added in synthesis to the N-terminal of the PNA, via an eg1 (8-amino-3,6-dioxoactanoic acid) linker. PNA-BPP conjugates were purified and verified by HPLC and MALDI-TOF mass spectrometric analysis (Supplementary Figure S1), as described previously (Christensen et al., 1995). All PNA-BPP handling was performed as described in detail (Goltermann and Nielsen, 2020).

Minimal inhibitory concentration

E. coli susceptibility to anti-DnaA PNA-BPPs was determined on cultures diluted to OD = 0.0002 by broth microdilution, using a Clinical and Laboratory Standards Institute (CLSI) protocol updated for PNA use, as described previously (Goltermann and Nielsen, 2020). Since PNA-BPPs adhere to polystyrene surfaces, this updated protocol includes the use of low-binding plastic, non-cation-adjusted Mueller–Hinton broth, alongside PNA-BPP stocks and dilution prepared in 0.4% BSA/0.02% acetic acid. MICs were determined with a BIOTEK™ Synergy H1 microplate reader (Agilent, Santa Clara, CA, USA).

Western blot analysis

Wild-type cells were grown exponentially in AB minimal medium supplemented with glucose and casamino acids, diluted to OD₄₅₀ = 0.01 and exposed to PNA-BPPs. Cells were collected and harvested after 3 h. Harvested cells were washed in 10-mM Tris-HCl pH 8 and 10-mM MgCl₂ and kept at -20°C. Samples were

heated at 95°C for 5 min and sonicated using a Branson 450 sonifier. Total protein content was quantified using Bradford Reagent (Sigma Aldrich), normalized to the same protein level (1–1.5 μ g) and separated using SDS-PAGE (Precast Gel: 10–20% Tris-HCl: Bio-Rad Inc., Copenhagen, Denmark) in an Xcell 4 SureLock™, Midi-Cell (ThermoFisher Scientific, Waltham, MA, USA). Samples were transferred to a polyvinylidene difluoride (PVDF) membrane (Whatman™, GE Healthcare, Chicago, IL, USA), using a semidry blotting apparatus (JKA Biotech, Denmark). DnaA protein was detected with polyclonal anti-DnaA antibodies (Charbon et al., 2021). The PVDF membrane was incubated with Enhanced Chemiluminescence (ECL) substrate (Bio-Rad) and the signal was detected using an ImageQuant LAS400 (GE Healthcare, Life Sciences). Quantification of Western blotting and analysis was performed using ImageJ software. A nonspecific band seen with the DnaA antibody was used as loading control and is included in the figures.

Inhibitor assay

The reporter strain (ALO5429) was grown overnight in AB minimal medium supplemented with glucose and casamino acids, and with appropriate antibiotics (40 μ g/mL of kanamycin, 20 μ g/mL of chloramphenicol, and 50 μ g/mL of streptomycin). The strain was diluted to 1–5 $\times 10^5$ CFU/mL and added as 90- μ l aliquots to a clear-bottomed black-sided 96-well plate already containing 10 μ l of DnaA-3-PNA at the desired range of concentrations. The plate was incubated for 18 h at 37°C, while continuously shaken at 220 rpm, in a BIOTEK™ Synergy H1 microplate reader. After 18 h, OD₄₅₀ and fluorescence (485-nm excitation and 528-nm emission) were measured in the BIOTEK™ Synergy H1 microplate reader. The fluorescence of each well was compared to the fluorescence of the untreated wells. A control strain (ALO5125) without the lambda *cI* gene carrying mini-chromosome pRNK6 was included in the experiments as reference for maximal green fluorescent protein (GFP) fluorescence.

Flow cytometry

Cell cycle parameters were determined by flow cytometry using an Apogee A10 instrument, as previously described (Lobner-Olesen et al., 1989). Samples for flow cytometry were taken from cultures prior to and following treatment with rifampicin/cephalexin. Briefly described, 1 mL of cell samples was centrifuged and fixed in 70% ethanol and 100- μ l 10-mM Tris buffer at pH 7.5 and then stored at 4°C. The number of origins per cell was determined from a sampled treated with rifampicin (300 μ g/ μ L) and cephalexin (36 μ g/ μ L) for 4 h prior to fixation. Rifampicin inhibits DNA replication indirectly through the inhibition of RNA synthesis; however, ongoing replication cycles will be completed, while cephalexin prevents cell division. Therefore, the number of chromosomes per cell will represent

the number of origins of replication present at the time of rifampicin/cephalexin addition.

In vivo visualization of the origin and terminus by fluorescence microscopy

Cells were washed and resuspended in 0.9% NaCl and kept on ice until mounted on microscope pads coated with a 1% agarose. Fluorescence microscopy was performed using an AxioImager Z1 microscope (Carl Zeiss MicroImaging, Inc., Jena, Germany), with a 100× objective and a Hamamatsu ORCA-ER C4742-80-12AG camera, as described previously (Charbon et al., 2014). Images were processed with ImageJ Software (Schneider et al., 2012; Schindelin et al., 2015).

DnaA depletion

Strain ALO8528 was grown exponentially in AB minimal medium supplemented with glycerol, casamino acids, and 10 µg/mL of tetracycline. At time T = 0, 1 mM of isopropyl beta-D-1 thiogalactopyranoside (IPTG) was added to the growth medium to initiate DnaA depletion. During depletion, the cultures were diluted in fresh pre-warmed medium containing IPTG.

Statistical analysis

GraphPad Prism (v.5, GraphPad Software) was used for graph illustrations and statistical analysis. The level of significance was evaluated by one-way analysis of variance (ANOVA), using Dunnett's multiple comparison test between non-treated samples and treated samples. The statistical significance level was set to a P value of ≤ 0.01 .

Results

DnaA-PNA inhibits cell growth in an *oriC*-dependent manner, through the inhibition of DnaA translation

To target *dnaA* mRNA translation, three anti-DnaA-PNAs were designed complementary to a 10-nucleotide region of the *dnaA* mRNA transcript, proximal to the ribosomal binding site and the GUG start codon (DnaA-1-, DnaA-2-, and DnaA-3-PNA). Each PNA was conjugated to the well-characterized lysine-rich (KFF)₃K BPP (Table 1). Note that this carrier peptide is degraded upon entry into the bacterial cell so that only PNA or KFF-PNA enters the bacterial cell (Yavari et al., 2021). Therefore, the BPP moiety is not considered a hindrance in the hybridization between PNA and its mRNA target. Antimicrobial activity was determined in wild-type *E. coli* cells (MG1655), and all anti-DnaA PNA-BPPs inhibited cell

growth at minimal inhibitory concentrations (MICs) of 2–4 µM (Table 1; Figure 1A; Supplementary Figure S2A). We decided to proceed with the DnaA-3-PNA which had a MIC of 2 µM, and a mismatch PNA control was designed based on its sequence, but with two bases interchanged (mismatch KFF). The mismatch KFF had a MIC of 16 µM (Table 1; Figure 1A) which is consistent with previous observations made from scrambled/mismatched PNA sequences of a similar length, indicating a degree of toxicity of PNA and/or the carrier peptide itself (Campion et al., 2021; Popella et al., 2022).

Western blot analysis revealed that DnaA protein levels were reduced by about 30% by DnaA-3-PNA treatment (Figure 1B; Supplementary Figure S2B) while the corresponding mismatch PNA did not significantly affect DnaA protein levels. The modest decrease in DnaA level should be seen in light of the stability of the protein with a half-life of >24 h (Torheim et al., 2000). Because samples for Western blots were taken at a much higher cell density (OD₄₅₀ = 0.01) than those used for MIC determinations (OD₆₀₀ = 0.0002), 8 µM of DnaA-3-PNA was used. The two other anti-DnaA-PNA, DnaA-1-PNA and DnaA-2-PNA, reduced the level of DnaA protein to about the same level as DnaA-3-PNA (Supplementary Figure S2B), strongly supporting the conclusion that anti-DnaA PNA-BPP specifically inhibits translation of the *dnaA* mRNA.

To show that growth inhibition was through the prevention of DnaA-mediated chromosome replication initiation at *oriC*, we tested anti-DnaA PNA-BPPs in a recently developed DnaA-inhibitor screen (Klitgaard and Løbner-Olesen, 2019). This assay utilizes *ΔrnhA*, *ΔoriC* *E. coli* cells, which initiate chromosome replication from *oriK* sites independent of DnaA and *oriC* (de Massy et al., 1984; Maduiké et al., 2014), in a process called *constitutive stable DNA replication* (cSDR) (Kogoma, 1997). The screening strain, ALO5429, contains a chromosomally encoded GFPmut2 under lambda P_R-promoter control and an *oriC*- and DnaA-dependent mini-chromosome (pRNK6) carrying a constitutively expressed lambda phage *cI* repressor gene. In this screen, any compound that inhibits the DnaA function or *oriC* strand opening, will lead to loss of the mini-chromosome and hence, the lambda CI repressor, which in turn results in an increase in fluorescence, without compromising cell viability. Cells treated with DnaA-3-PNA exhibited a concentration-dependent increase in relative fluorescence, indicating that replication of the mini-chromosome was inhibited (Figure 1C). Again, the two other anti-DnaA-PNA, DnaA-1-PNA and DnaA-2-PNA, behaved as DnaA-3-PNA (Supplementary Figure S2C). The degree of inhibition was similar to that observed by the expression of a cyclic DnaA domain I-derived peptide known to inhibit DnaA function (Kjelstrup et al., 2013). In summary, these data are consistent with the conclusion that DnaA-3-PNA specifically targets DnaA protein expression and inhibits bacterial growth in an *oriC*-dependent manner. Note that bacterial sensitivity to a reduction in the synthesis of different essential proteins varies, and therefore, MIC values are not necessarily proportional to their reduction level (Popella et al., 2022).

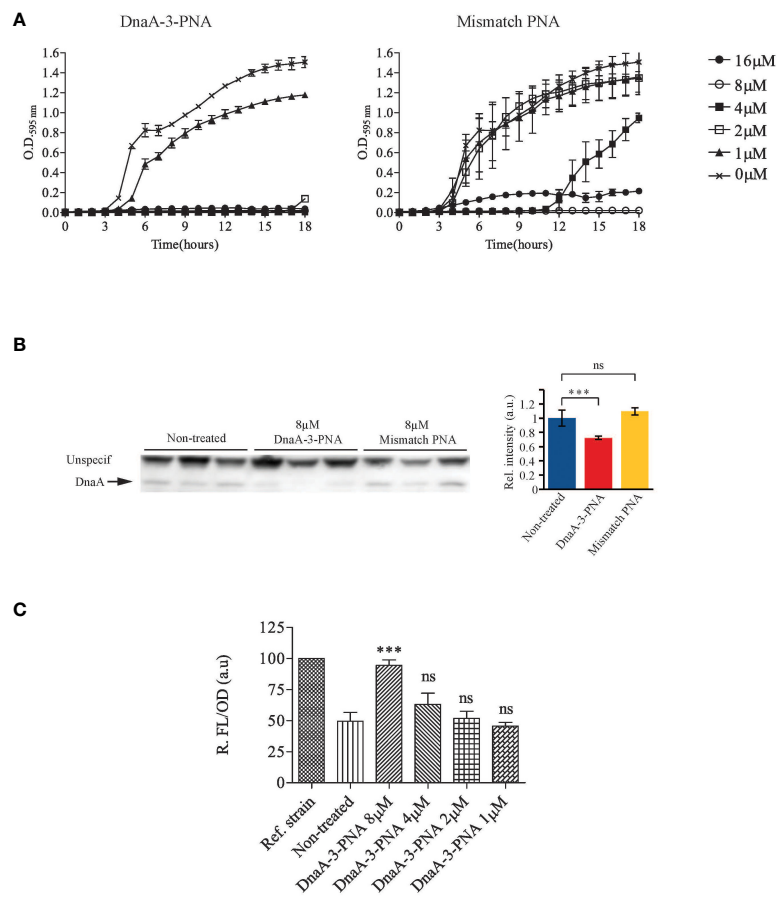


FIGURE 1
 DnaA-3-PNA inhibits cell growth, through the inhibition of DnaA translation. **(A)** Anti-DnaA PNA-BPPs inhibits bacterial growth. Overnight cultures of wild-type cells were diluted to 10⁵ cfu/mL in MHB-I and then appropriate concentrations of the indicated PNA-BPPs were added. Cells were incubated at 37°C for 18 h, while turbidity was measured at OD₅₉₅. **(B)** Anti-DnaA PNA-BPPs inhibits *dnaA* translation. Cell extracts for protein immunoblotting was collected from cells growing exponentially in AB minimal medium supplemented with glucose and casamino acids, treated with 8 μM of either DnaA-3-PNA or 2x-mismatch KFF. Cell extracts were collected at OD₄₅₀ = 0.4-0.5 and proteins were separated in SDS-PAGE gels. DnaA protein was detected by immunoblotting. The nonspecific band seen with the DnaA antibody was used as loading control. Relative band intensity relative to wild type is shown as a bar graph representing the mean ± SD based on the band intensity; ns, not significant; ***, P<0.01. **(C)** DnaA-3-PNA specificity confirmed in an *oriC*/DnaA specific inhibitor screen. Overnight cultures of ALO5429 were diluted to 10⁵ cfu/mL in AB minimal medium supplemented with glucose and casamino acids and then appropriate concentrations of DnaA-3-PNA were added. Cells were incubated at 37°C for 18 h. The cells were washed in 10% NaCl and then turbidity and fluorescence were measured. The reference strain ALO5125 does not contain the *cl* carrying mini-chromosome pRNK6 and hence, represent the maximal fluorescence obtainable in this system.

Anti-DnaA PNA-peptides prevent the initiation of chromosome replication

Flow cytometry was used to assess the effect of DnaA-3-PNA on chromosome replication (Lobner-Olesen et al., 1989). During growth in minimal medium supplemented with glucose and casamino acids, untreated cells were uniform in mass and DNA content, with the majority containing four chromosome equivalents, after being treated with rifampicin and cephalixin to block replication initiation and cell division, respectively (Figure 2A). These chromosome equivalents represent the number of chromosomal origins (*oriC*) in each cell, at the time of drug treatment (Boye and Lobner-Olesen, 1991). The average number of *origins*/cell was 4.7 (Figure 2A). Cells treated for 2 h with DnaA-3-PNA had a lower DNA content, with the majority of

cells containing one fully replicated chromosome and a few cells with two fully replicated chromosomes.

The appearance of fully replicated chromosomes in the absence of rifampicin/cephalexin treatment is usually observed in cells entering stationary phase and ceasing chromosome replication (Boye and Lobner-Olesen, 1991). Because the optical density of the DnaA-3-PNA treated cultures never exceeded OD₄₅₀ = 0.2, present data suggest that cells never entered stationary phase but that treatment with DnaA-3-PNA led to cessation of chromosome replication initiation and continued cell division, eventually generating cells containing one fully replicated chromosome (Figure 2A). The increase in cell size upon 2-h treatment with DnaA-3-PNA also suggests that once formed, the 1-chromosome cells continue to increase in size without further initiations (Figure 2A). A similar pattern was observed for *dnaA46* cells shifted to non-permissive

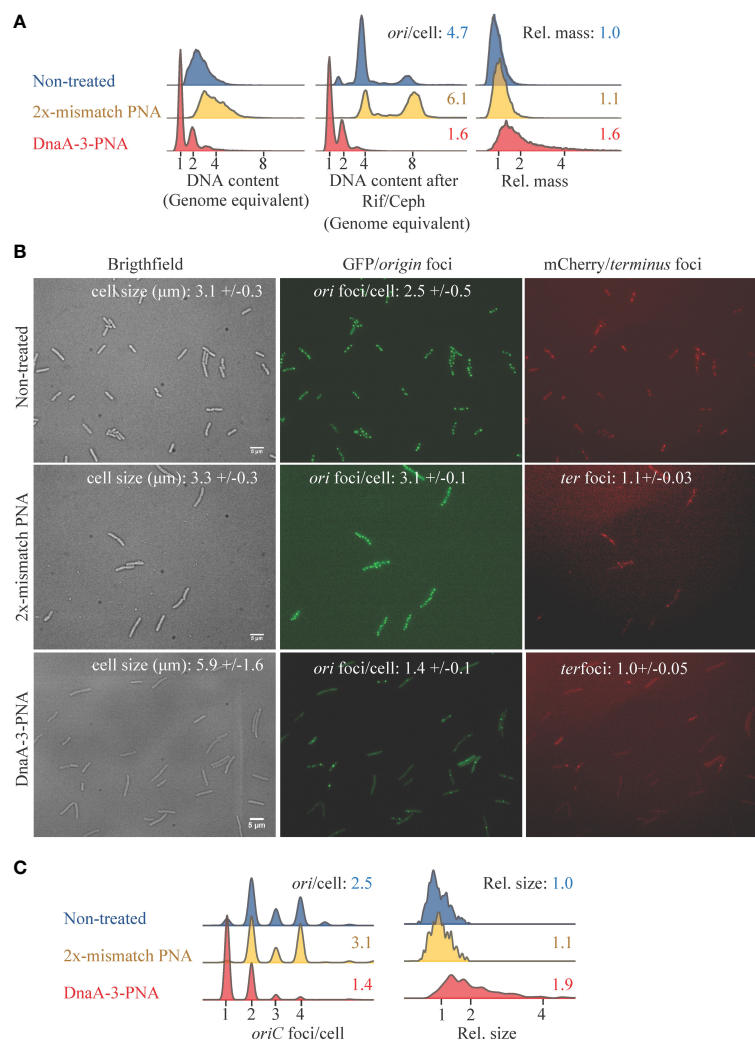


FIGURE 2

DnaA-3-PNA inhibits initiation of chromosome replication. **(A)** Cell-cycle analysis of cells treated with anti-DnaA PNA-BPPs. MG1655 were grown exponentially in AB minimal medium supplemented with glucose and casamino acids, diluted to $OD_{450} = 0.005$, and exposed to DnaA-3-PNA or mismatch KFF ($10 \mu\text{M}$) for 2 h before sample collection for flow cytometry. The following are shown: cell size distributions (a.u.) of exponentially grown cells, DNA content of cells, and DNA content of cells treated with rifampicin and cephalixin for chromosome replication to be completed. Each panel represents 30–50,000 cells. **(B)** Cell morphology and localization of *ori* and *ter* regions of DnaA-3-PNA and 2x-mismatch KFF-treated cells. Strain ALO4223 was grown exponentially in AB minimal medium supplemented with glucose and casamino acids, diluted to $OD_{450} = 0.005$, and exposed to DnaA-3-PNA or 2x-mismatch KFF ($10 \mu\text{M}$) or left untreated for 2 (h) Scale bar is $5 \mu\text{m}$. Cell size and cell cycle parameters given as *ori* foci/cell and *ter* foci were inserted. These values were based on pooled counts of 2–3 independent determinations: Non-treated ($n = 256, 211$, and 128); DnaA-3-PNA ($n = 222, 211$, and 151); mismatch-PNA ($n = 168$ and 117). **(C)** *oriC* foci/cell and relative cell size were determined for each growth/treatment condition and visualized as histograms.

temperature (see below). Consequently, treatment with rifampicin and cephalixin did not alter the DNA distribution of DnaA-3-PNA-treated cells (Figure 2A). The average cell size increased when cells were treated with DnaA-3-PNA for 2 h (Figure 2) and continued to increase upon longer periods of treatment (Supplementary Figure S3). The decrease in average *origins*/cell and increase in cell size led to an overall decrease in origin concentration (*origins*/cell mass) for cells treated with DnaA-3-PNA. Cells treated with the mismatch PNA resembled untreated cells. Collectively, these observations strongly suggest that cells treated with DnaA-3-PNA fail to initiate new rounds of chromosome replication, which results in the appearance of fully replicated chromosomes and a decrease in

the average number of *origins*/cell. This leads to a delay in cell division and an increase in relative cell mass.

We proceeded to directly visualize the effect of DnaA-3-PNA in an *ori* and *ter* tagged strain, as previously described (Charbon et al., 2014). The non-treated cells were uniform in appearance, and the majority of cells observed contained two or four origin foci per cell with a mean of 2.5 (Figures 2B, C). Cells treated with DnaA-3-PNA for 2 h became heterogeneous in size, with the majority of cells being enlarged. The majority of cells contained one *origin* foci/cell only (Figures 2B, C). The average number of *ter* foci per cell remained close to one irrespective of DnaA-3-PNA treatment (Figure 2B). Cells treated with mismatch PNA were very similar to non-treated cells (Figures 2B, C).

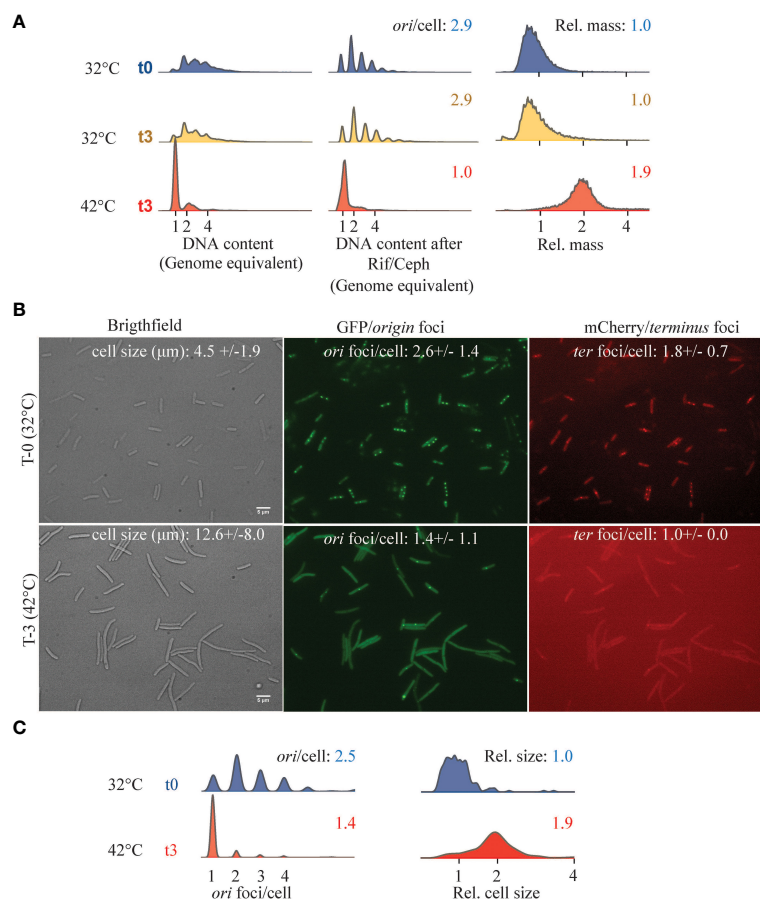


FIGURE 3

Cell cycle parameters of DnaA46 mutants at non-permissive temperature. ALO8290 cells were grown exponentially in AB minimal medium supplemented with glucose and casamino acids, diluted to $OD_{450} = 0.05$ ($T = 0$), and then split with one half remaining at 32°C and the other half was incubated at 42°C. At the indicated time points, samples were collected for flow cytometry and fluorescence microscopy. **(A)** Histograms of cell size distribution (a.u.), DNA content, and DNA content of cells treated with rifampicin and cephalixin. Each panel represents 30–80,000 cell events. **(B)** *In vivo* visualization of *ori* and *ter* foci, alongside phase contrast images at 32°C ($T = 0$) and following 3 h at 42°C ($T = 3$). Cell size and cell cycle parameters given as *ori* foci/cell and *ter* foci/cell were inserted. Cell length and foci/cell were determined based on $n = 197$ –545 counted cells of each condition, individually (32°C T_0 ; $n = 234$) and (42°C; $n = 307$). Scale bar is 5 μm . **(C)** Relative cell size and *ori* foci/cell were determined for each growth condition indicated and visualized as histograms.

To allow comparison of DnaA-3-PNA-treated wild-type cells to cells limited in activity or amount of the DnaA protein, we used a thermo-sensitive *dnaA* mutant (DnaA46) and a DnaA-depletion assay, respectively.

The temperature-sensitive DnaA46 protein contains A184V and H252Y substitutions, both in the domain responsible for ATP binding (Carr and Kaguni, 1996). Consequently, the DnaA46 protein binds neither ATP nor ADP at any temperature, yet the DnaA protein is functional and is capable of initiating DNA replication from *oriC* at permissive temperature, albeit with a loss of coordination of initiations (Skarstad et al., 1986, 1988). When DnaA46 cells were shifted to non-permissive temperature, cells ceased to initiate new rounds of chromosome replication, which resulted in the appearance of fully replicated chromosomes and a decrease in the average number of *origins*/cell (Figure 3A). As a consequence of the cessation of initiation of DNA replication, cell division was delayed, leading to an increase in relative cell mass (Figure 3A). Similarly, when visualized *in vivo*, cells shifted to non-

permissive temperature became elongated and contained mainly one *origin* foci/cell (Figures 3B, C).

To deplete cells for DnaA, we used $\Delta dnaA$ mutant cells carrying the *dnaA* gene expressed from its native promoter on a low copy number R1-based plasmid. The cells also carried the pSC101-derived plasmid pKG339, which, upon IPTG induction, expressed the antisense RNA *CopA* that inhibits the R1 plasmid replication (Jensen et al., 1995). Upon IPTG addition, the replication of the R1-based plasmid carrying *dnaA* ceases while cell growth and division continue (Jensen et al., 1995). Over time, the plasmid carrying *dnaA* is lost, leading to dilution of the DnaA protein. We observed that IPTG induction resulted in the appearance of fully replicated chromosomes (Figure 4), a phenotype similar to that of DnaA46 cells at non-permissive temperature and to DnaA-3-PNA-treated cells. However, further treatment with rifampicin and cephalixin revealed that replication cessation by depletion was somewhat partial (Figure 4). DnaA depletion also resulted in an increased cell size and hence, a

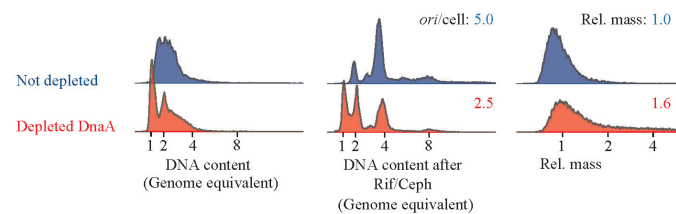


FIGURE 4

Cell-cycle profile of DnaA depleted cells. Strain ALO8528 was grown exponentially in AB minimal medium supplemented with glycerol, casamino acids, and tetracycline. At $T = 0$, the culture was split, one portion with 1-mM IPTG added to initiate DnaA depletion and the other portion was left untreated. Cells were propagated for approximately 12 mass doublings in the same medium while diluting cells whenever OD_{450} exceeded 0.2. Finally, samples were collected at $OD_{450} = 0.2$ for flow cytometry analysis. Each panel represents 30–80,000 cells.

reduced average number of *origins*/cell. These findings further support that treatment with anti-DnaA PNA does indeed result in DnaA depletion leading to growth inhibition.

Discussion

DnaA as an antimicrobial drug target

As a conserved and essential gene, DnaA has long been considered an excellent antimicrobial drug target (Grimwade and Leonard, 2019). The DnaA protein itself can be targeted at multiple levels such as DnaA ATPase activity, oligomerization, loading of the helicase or binding to *oriC*, and several *in vitro* screens have been developed to identify molecules that affect these activities (Sasaki et al., 1994; Johnsen et al., 2010; Charbon et al., 2018a; Klitgaard and Løbner-Olesen, 2019). An *in vitro* non-competitive inhibitor of ATP binding (3-Acetoxy-2,2'-bi-1H-indol) was discovered in 1994 (Sasaki et al., 1994), showing a IC_{50} of 0.04-mM in a DnaA-ATP binding assay. A derivative of this compound (3-[N-(11-carboxyundecyl)] carbamoylmethoxy-2,2'-bi-1H-indol) was later found to be more potent, with an IC_{50} value of 7 μ M (Mizushima et al., 1996). However, the antibacterial activity and specificity of these drugs have never been reported. The expression of a cyclic DnaA domain I-derived peptide known to specifically inhibit DnaA oligomerization has been shown to arrest cellular growth (Kjelstrup et al., 2013). However, due to poor cell penetration of peptides, it remains to be seen whether the cyclic peptide could be used as an actual drug when provided extracellularly. Other attempts have been made using cell-based screens to find drugs that work in cell culture (Fossum et al., 2008; Johnsen et al., 2010; Charbon et al., 2018a; Klitgaard and Løbner-Olesen, 2019). However, none of the molecules identified were found to affect DnaA, indicating that the protein may be difficult to target. It is likely that drugs that affect DnaA activity would mimic ATP and in principle, target other ATP-binding proteins as well. Moreover, small molecules affecting protein–protein interaction are expected to be difficult to find (Grimwade and Leonard, 2019). The apparent ease of selection of intra or extragenic suppressor mutations further complicates the screening process (Charbon et al., 2018b). Targeting the expression of DnaA can circumvent these hurdles because the loss of/reduction in DnaA protein level results in the cessation of chromosome replication and inhibition of cell growth as

observed here. Note that the effect of DnaA translation knockdown is not limited to DNA replication as other essential cellular processes may be affected as well (Menikpurage et al., 2021) since DnaA is also a global transcription factor. DnaA has been linked to the regulation of several genes encoding enzymes pivotal for essential processes such as deoxyribonucleotide synthesis through *nrdAB* (Augustin et al., 1994; Gon et al., 2006; Olliver et al., 2010; Babu et al., 2017) and *guaB* (Tesfa-Selase and Drabble, 1992), DNA repair, through *uvrB* (Wurihan et al., 2018) and *polA* (Quinones et al., 1997), as well as playing a role in stress survival (Sass et al., 2022).

The present antisense compounds inhibited MG1655 growth at approximately 2 μ M and demonstrated that *dnaA* translation is a functional antisense PNA target. However, on the road toward new antibiotics, a systematic structure activity approach identifying the most sensitive PNA sequence target sites in the *dnaA* mRNA as well as the most effective BPP must be carried out in order to optimize potency, specificity, cytotoxicity, and biostability, and eventually *in vivo* properties. Indeed, a large variety of arginine/guanidinium BPPs that also allow *in vivo* efficacy studies have already been identified (Goltermann et al., 2019; Frimodt-Moller et al., 2021; Iubatti et al., 2022).

An antimicrobial effect has previously been observed for the control PNA-peptides with scrambled/mismatch sequences, which have been in part attributed to the activation of envelope stress response pathways (Popella et al., 2022).

Conclusion

Lysine-rich (KFF)₃K PNA-BPPs designed to target the initiation of DNA replication, by inhibiting the expression of the initiator protein DnaA, exhibited micromolar antibacterial activity toward MG1655, and the treated cells had decreased DnaA protein levels that led to growth inhibition dependent on *oriC*. Furthermore, cells treated with DnaA-3-PNA exhibited hallmarks associated with chromosome replication inhibition similar to that observed when DnaA activity was compromised (*i.e.* in DnaA46 cells at non-permissive temperature), or when DnaA was depleted. Collectively, the data provide strong genetic and phenotypic evidence for the inhibition of initiation of chromosome replication in cells where *dnaA* translation was inhibited by specific PNA-BPP, and thus, identifies *dnaA* as a *bona fide* antibacterial target using antisense-PNA technology.

Data availability statement

The original contributions presented in the study are included in the article/Supplementary Material. Further inquiries can be directed to the corresponding author.

Author contributions

CC: Conceptualization, Writing – original draft, Writing – review & editing, Formal analysis, Investigation, Methodology. GC: Conceptualization, Investigation, Methodology, Writing – original draft, Writing – review & editing. PN: Conceptualization, Funding acquisition, Investigation, Methodology, Project administration, Resources, Writing – original draft, Writing – review & editing. AL: Conceptualization, Project administration, Resources, Supervision, Writing – original draft, Writing – review & editing.

Funding

The author(s) declare that financial support was received for the research, authorship, and/or publication of this article. This research was funded through a Challenge program (NNF16OC0021700) from the Novo Nordisk Foundation, by Grant DNRF120 from the Danish National Research Foundation and by Grant 39854 from the Villum Foundation.

References

- Augustin, L. B., Jacobson, B. A., and Fuchs, J. A. (1994). Escherichia coli Fis and DnaA proteins bind specifically to the nrd promoter region and affect expression of an nrd-lac fusion. *J. Bacteriol.* 176, 378–387. doi: 10.1128/jb.176.2.378-387.1994
- Babu, V. M. P., Itsko, M., Baxter, J. C., Schaaper, R. M., and Sutton, M. D. (2017). Insufficient levels of the nrdAB-encoded ribonucleotide reductase underlie the severe growth defect of the Delta hda E. coli strain. *Mol. Microbiol.* 104, 377–399. doi: 10.1111/mmi.13632
- Botello, E., and Nordstrom, K. (1998). Effects of chromosome underreplication on cell division in Escherichia coli. *J. Bacteriol.* 180, 6364–6374. doi: 10.1128/JB.180.23.6364-6374.1998
- Boye, E., and Lobner-Olesen, A. (1991). Bacterial growth control studied by flow cytometry. *Res. Microbiol.* 142, 131–135. doi: 10.1016/0923-2508(91)90020-B
- Bramhill, D., and Kornberg, A. (1988). Duplex opening by dnaA protein at novel sequences in initiation of replication at the origin of the E. coli chromosome. *Cell* 52, 743–755. doi: 10.1016/0092-8674(88)90412-6
- Campion, C., Charbon, G., Thomsen, T. T., Nielsen, P. E., and Lobner-Olesen, A. (2021). Antisense inhibition of the Escherichia coli NrdAB aerobic ribonucleotide reductase is bactericidal due to induction of DNA strand breaks. *J. Antimicrob. Chemother.* 76, 2802–2814. doi: 10.1093/jac/dkab305
- Carr, K. M., and Kaguni, J. M. (1996). The A184V missense mutation of the dnaA5 and dnaA46 alleles confers a defect in ATP binding and thermostability in initiation of Escherichia coli DNA replication. *Mol. Microbiol.* 20, 1307–1318. doi: 10.1111/j.1365-2958.1996.tb02649.x
- Charbon, G., Bjorn, L., Mendoza-Chamizo, B., Frimodt-Moller, J., and Lobner-Olesen, A. (2014). Oxidative DNA damage is instrumental in hyperreplication stress-induced inviability of Escherichia coli. *Nucleic Acids Res.* 42, 13228–13241. doi: 10.1093/nar/gku1149
- Charbon, G., Klitgaard, R. N., Liboriussen, C. D., Thulstrup, P. W., Maffioli, S. I., Donadio, S., et al. (2018a). Iron chelation increases the tolerance of Escherichia coli to hyper-replication stress. *Sci. Rep.* 8, 10550. doi: 10.1038/s41598-018-28841-9
- Charbon, G., Mendoza-Chamizo, B., Campion, C., Li, X., Jensen, P. R., Frimodt-Moller, J., et al. (2021). Energy starvation induces a cell cycle arrest in Escherichia coli by triggering degradation of the DnaA initiator protein. *Front. Mol. Biosci.* 8. doi: 10.3389/fmolb.2021.629953
- Charbon, G., Riber, L., and Lobner-Olesen, A. (2018b). Countermeasures to survive excessive chromosome replication in Escherichia coli. *Curr. Genet.* 64, 71–79. doi: 10.1007/s00294-017-0725-4
- Christensen, L., Fitzpatrick, R., Gildea, B., Petersen, K. H., Hansen, H. F., Koch, T., et al. (1995). Solid-phase synthesis of peptide nucleic acids. *J. Pept. Sci.* 1, 175–183. doi: 10.1002/psc.310010304
- Clark, D. J., and Maaløe, O. (1967). DNA replication and the division cycle in Escherichia coli. *J. Mol. Biol.* 23, 99–122. doi: 10.1016/S0022-2836(67)80070-6
- de Massy, B., Fayet, O., and Kogoma, T. (1984). Multiple origin usage for DNA replication in sdrA(rnh) mutants of Escherichia coli K-12. Initiation in the absence of oriC. *J. Mol. Biol.* 178, 227–236. doi: 10.1016/0022-2836(84)90141-4
- Dryselius, R., Aswasti, S. K., Rajarao, G. K., Nielsen, P. E., and Good, L. (2003). The translation start codon region is sensitive to antisense PNA inhibition in Escherichia coli. *Oligonucleotides* 13, 427–433. doi: 10.1089/154545703322860753
- Egholm, M., Buchardt, O., Christensen, L., Behrens, C., Freier, S. M., Driver, D. A., et al. (1993). PNA hybridizes to complementary oligonucleotides obeying the Watson-Crick hydrogen-bonding rules. *Nature* 365, 566–568. doi: 10.1038/365566a0
- Erzberger, J. P., Mott, M. L., and Berger, J. M. (2006). Structural basis for ATP-dependent DnaA assembly and replication-origin remodeling. *Nat. Struct. Mol. Biol.* 13, 676–683. doi: 10.1038/nsmb1115
- Fossum, S., De Pascale, G., Weigel, C., Messer, W., Donadio, S., and Skarstad, K. (2008). A robust screen for novel antibiotics: specific knockout of the initiator of bacterial DNA replication. *FEMS Microbiol. Lett.* 281, 210–214. doi: 10.1111/fml.2008.281.issue-2
- Frimodt-Møller, J., Boesen, T. O., Charbon, G., and Lobner-Olesen, A. (2024). “Chapter 14 - Bacterial chromosomes and their replication,” in *Molecular Medical Microbiology (Third Edition)*. Eds. Y.-W. Tang, M. Y. Hindiyeh, D. Liu, A. Sails, P.

Acknowledgments

The authors thank Jolanta Barbara Ludvigsen for the PNA synthesis.

Conflict of interest

The authors declare that the research was conducted in the absence of any commercial or financial relationships that could be construed as a potential conflict of interest.

Publisher's note

All claims expressed in this article are solely those of the authors and do not necessarily represent those of their affiliated organizations, or those of the publisher, the editors and the reviewers. Any product that may be evaluated in this article, or claim that may be made by its manufacturer, is not guaranteed or endorsed by the publisher.

Supplementary material

The Supplementary Material for this article can be found online at: <https://www.frontiersin.org/articles/10.3389/frabi.2024.1384390/full#supplementary-material>

- Spearman and J.-R. Zhang (London, United Kingdom: Academic Press), 279–307. doi: 10.1016/b978-0-12-818619-0.00007-1
- Frimodt-Moller, J., Koulouktsis, A., Charbon, G., Otterlei, M., Nielsen, P. E., and Lobner-Olesen, A. (2021). Activating the Cpx response induces tolerance to antisense PNA delivered by an arginine-rich peptide in *Escherichia coli*. *Mol. Ther. Nucleic Acids* London, UK, 25, 444–454. doi: 10.1016/j.omtn.2021.06.009
- Ghosal, A. (2017). Peptide nucleic acid antisense oligomers open an avenue for developing novel antibacterial molecules. *J. Infect. Dev. Ctries* 11, 212–214. doi: 10.3855/jidc.9159
- Goltermann, L., and Nielsen, P. E. (2020). PNA antisense targeting in bacteria: determination of antibacterial activity (MIC) of PNA-peptide conjugates. *Methods Mol. Biol.* 2105, 231–239. doi: 10.1007/978-1-0716-0243-0_14
- Goltermann, L., Yavari, N., Zhang, M., Ghosal, A., and Nielsen, P. E. (2019). PNA length restriction of antibacterial activity of peptide-PNA conjugates in *Escherichia coli* through effects of the inner membrane. *Front. Microbiol.* 10. doi: 10.3389/fmicb.2019.01032
- Gon, S., Camara, J. E., Klungsoyr, H. K., Crooke, E., Skarstad, K., and Beckwith, J. (2006). A novel regulatory mechanism couples deoxyribonucleotide synthesis and DNA replication in *Escherichia coli*. *EMBO J.* 25, 1137–1147. doi: 10.1038/sj.emboj.7600990
- Good, L., Awasthi, S. K., Dryselius, R., Larsson, O., and Nielsen, P. E. (2001). Bactericidal antisense effects of peptide-PNA conjugates. *Nat. Biotechnol.* 19, 360–364. doi: 10.1038/86753
- Good, L., and Nielsen, P. E. (1998). Antisense inhibition of gene expression in bacteria by PNA targeted to mRNA. *Nat. Biotechnol.* 16, 355–358. doi: 10.1038/nbt0498-355
- Good, L., Sandberg, R., Larsson, O., Nielsen, P. E., and Wahlestedt, C. (2000). Antisense PNA effects in *Escherichia coli* are limited by the outer-membrane LPS layer. *Microbiology* 146, 2665–2670. doi: 10.1099/00221287-146-10-2665
- Grimwade, J. E., and Leonard, A. C. (2019). Blocking the trigger: inhibition of the initiation of bacterial chromosome replication as an antimicrobial strategy. *Antibiotics (Basel)* 8, 1–17. doi: 10.3390/antibiotics8030111
- Hansen, F. G., and Atlung, T. (2018). The DnaA tale. *Front. Microbiol.* 9. doi: 10.3389/fmicb.2018.00319
- Ingmer, H., and Atlung, T. (1992). Expression and regulation of a *dnaA* homologue isolated from *Pseudomonas putida*. *Mol. Gen. Genet.* 232, 431–439. doi: 10.1007/BF00266248
- Tubatti, M., Gabas, I. M., Cavaco, L. M., Mood, E. H., Lim, E., Bonanno, F., et al. (2022). Antisense peptide nucleic acid-diaminobutanoic acid dendron conjugates with SbmA-independent antimicrobial activity against gram-negative bacteria. *ACS Infect. Dis* 8, 1098–1106. doi: 10.1021/acinfedcis.2c00089
- Jensen, R. B., Grohmann, E., Schwab, H., Diaz-Orejas, R., and Gerdes, K. (1995). Comparison of *cfd* of F, *parDE* of RP4, and *parD* of R1 using a novel conditional replication control system of plasmid R1. *Mol. Microbiol.* 17, 211–220. doi: 10.1111/j.1365-2958.1995.mmi_17020211.x
- Johnsen, L., Weigel, C., von Kries, J., Moller, M., and Skarstad, K. (2010). A novel DNA gyrase inhibitor rescues *Escherichia coli* *dnaAcos* mutant cells from lethal hyperinitiation. *J. Antimicrob. Chemother.* 65, 924–930. doi: 10.1093/jac/dkq071
- Katayama, T., Kasho, K., and Kawakami, H. (2017). The DnaA cycle in *Escherichia coli*: activation, function and inactivation of the initiator protein. *Front. Microbiol.* 8. doi: 10.3389/fmicb.2017.02496
- Kjelstrup, S., Hansen, P. M., Thomsen, L. E., Hansen, P. R., and Lobner-Olesen, A. (2013). Cyclic peptide inhibitors of the beta-sliding clamp in *Staphylococcus aureus*. *PLoS One* 8, e72273. doi: 10.1371/journal.pone.0072273
- Klitgaard, R. N., and Lobner-Olesen, A. (2019). A novel fluorescence-based screen for inhibitors of the initiation of DNA replication in bacteria. *Curr. Drug Discovery Technol.* 16, 272–277. doi: 10.2174/1570163815666180423115514
- Kogoma, T. (1997). Stable DNA replication: interplay between DNA replication, homologous recombination, and transcription. *Microbiol. Mol. Biol. Rev.* 61, 212–238. doi: 10.1128/mmr.61.2.212-238.1997
- Lee, H. T., Kim, S. K., and Yoon, J. W. (2019). Antisense peptide nucleic acids as a potential anti-infective agent. *J. Microbiol.* 57, 423–430. doi: 10.1007/s12275-019-8635-4
- Lobner-Olesen, A., Boye, E., and Marinus, M. G. (1992). Expression of the *Escherichia coli* *dam* gene. *Mol. Microbiol.* 6, 1841–1851. doi: 10.1111/j.1365-2958.1992.tb01356.x
- Lobner-Olesen, A., Skarstad, K., Hansen, F. G., von Meyenburg, K., and Boye, E. (1989). The DnaA protein determines the initiation mass of *Escherichia coli* K-12. *Cell* 57, 881–889. doi: 10.1016/0092-8674(89)90802-7
- Maduik, N. Z., Tehranchi, A. K., Wang, J. D., and Kreuzer, K. N. (2014). Replication of the *Escherichia coli* chromosome in RNase HI-deficient cells: multiple initiation regions and fork dynamics. *Mol. Microbiol.* 91, 39–56. doi: 10.1111/mmi.12440
- Menikpurage, I. P., Woo, K., and Mera, P. E. (2021). Transcriptional activity of the bacterial replication initiator DnaA. *Front. Microbiol.* 12. doi: 10.3389/fmicb.2021.662317
- Mizushima, T., Sasaki, S., Ohishi, H., Kobayashi, M., Katayama, T., Miki, T., et al. (1996). Molecular design of inhibitors of *in vitro* *oriC* DNA replication based on the potential to block the ATP binding of DnaA protein. *J. Biol. Chem.* 271, 25178–25183. doi: 10.1074/jbc.271.41.25178
- Narenji, H., Gholizadeh, P., Aghazadeh, M., Rezaee, M. A., Asgharzadeh, M., and Kafil, H. S. (2017). Peptide nucleic acids (PNAs): currently potential bactericidal agents. *BioMed. Pharmacother.* 93, 580–588. doi: 10.1016/j.biopha.2017.06.092
- Nielsen, P. E., Egholm, M., Berg, R. H., and Buchardt, O. (1991). Sequence-selective recognition of DNA by strand displacement with a thymine-substituted polyamide. *Science* 254, 1497–1500. doi: 10.1126/science.1962210
- Olliver, A., Saggiaro, C., Herrick, J., and Sclavi, B. (2010). DnaA-ATP acts as a molecular switch to control levels of ribonucleotide reductase expression in *Escherichia coli*. *Mol. Microbiol.* 76, 1555–1571. doi: 10.1111/j.1365-2958.2010.07185.x
- Ozaki, S., Kawakami, H., Nakamura, K., Fujikawa, N., Kagawa, W., Park, S. Y., et al. (2008). A common mechanism for the ATP-DnaA-dependent formation of open complexes at the replication origin. *J. Biol. Chem.* 283, 8351–8362. doi: 10.1074/jbc.M708684200
- Popella, L., Jung, J., Do, P. T., Hayward, R. J., Barquist, L., and Vogel, J. (2022). Comprehensive analysis of PNA-based antisense antibiotics targeting various essential genes in uropathogenic *Escherichia coli*. *Nucleic Acids Res.* 50, 6435–6452. doi: 10.1093/nar/gkac362
- Quinones, A., Wandt, G., Kleinstaub, S., and Messer, W. (1997). DnaA protein stimulates *polA* gene expression in *Escherichia coli*. *Mol. Microbiol.* 23, 1193–1202. doi: 10.1046/j.1365-2958.1997.2961658.x
- Saorbach, J., Sabale, P. M., and Winsinger, N. (2019). Peptide nucleic acid (PNA) and its applications in chemical biology, diagnostics, and therapeutics. *Curr. Opin. Chem. Biol.* 52, 112–124. doi: 10.1016/j.cbpa.2019.06.006
- Sakiyama, Y., Nagata, M., Yoshida, R., Kasho, K., Ozaki, S., and Katayama, T. (2022). Concerted actions of DnaA complexes with DNA-unwinding sequences within and flanking replication origin *oriC* promote DnaB helicase loading. *J. Biol. Chem.* 298, 102051. doi: 10.1016/j.jbc.2022.102051
- Sasaki, S., Mizushima, T., Hashimoto, T., Maeda, M., and Sekimizu, K. (1994). 3-Acetoxy-2,2'-Bi-1h-Indol as a novel inhibitor of ATP binding to DnaA, the protein initiating chromosomal replication in *Escherichia coli*. *Bioorg. Medicinal Chem. Lett.* 4, 1771–1774. doi: 10.1016/S0960-894X(00)80378-9
- Sass, T. H., Ferrazzoli, A. E., and Lovett, S. T. (2022). DnaA and SspA regulation of the *iraD* gene of *Escherichia coli*: an alternative DNA damage response independent of LexA/RecA. *Genetics* 221, 1–12. doi: 10.1093/genetics/iyac062
- Schindelin, J., Rueden, C. T., Hiner, M. C., and Eliceiri, K. W. (2015). The ImageJ ecosystem: An open platform for biomedical image analysis. *Mol. Reprod. Dev.* 82, 518–529. doi: 10.1002/mrd.22489
- Schneider, C. A., Rasband, W. S., and Eliceiri, K. W. (2012). NIH Image to ImageJ: 25 years of image analysis. *Nat. Methods* 9, 671–675. doi: 10.1038/nmeth.2089
- Sekimizu, K., Bramhill, D., and Kornberg, A. (1987). ATP activates *dnaA* protein in initiating replication of plasmids bearing the origin of the *E. coli* chromosome. *Cell* 50, 259–265. doi: 10.1016/0092-8674(87)90221-2
- Simmons, L. A., Breier, A. M., Cozzarelli, N. R., and Kaguni, J. M. (2004). Hyperinitiation of DNA replication in *Escherichia coli* leads to replication fork collapse and inviability. *Mol. Microbiol.* 51, 349–358. doi: 10.1046/j.1365-2958.2003.03842.x
- Skarstad, K., Boye, E., and Steen, H. B. (1986). Timing of initiation of chromosome replication in individual *Escherichia coli* cells. *EMBO J.* 5, 1711–1717. doi: 10.1002/emj.1986.5.issue-7
- Skarstad, K., von Meyenburg, K., Hansen, F. G., and Boye, E. (1988). Coordination of chromosome replication initiation in *Escherichia coli*: effects of different *dnaA* alleles. *J. Bacteriol.* 170, 852–858. doi: 10.1128/jb.170.2.852-858.1988
- Tesfa-Selase, F., and Drabble, W. T. (1992). Regulation of the *gua* operon of *Escherichia coli* by the DnaA protein. *Mol. Gen. Genet.* 231, 256–264. doi: 10.1007/BF00279799
- Torheim, N. K., Boye, E., Lobner-Olesen, A., Stokke, T., and Skarstad, K. (2000). The *Escherichia coli* SeqA protein destabilizes mutant DnaA204 protein. *Mol. Microbiol.* 37, 629–638. doi: 10.1046/j.1365-2958.2000.02031.x
- Wojciechowska, M., Rownicki, M., Mieczkowski, A., Miskiewicz, J., and Trylska, J. (2020). Antibacterial peptide nucleic acids-facts and perspectives. *Molecules* 25, 1–22. doi: 10.3390/molecules25030559
- Wolanski, M., Donczew, R., Zawilak-Pawlik, A., and Zakrzewska-Czerwinska, J. (2014). *oriC*-encoded instructions for the initiation of bacterial chromosome replication. *Front. Microbiol.* 5, 1–22. doi: 10.3389/fmicb.2014.00735
- Wurihan, Gezi, Brambilla, E., Wang, S., Sun, H., Fan, L., et al. (2018). DnaA and LexA Proteins Regulate Transcription of the *uvrB* Gene in *Escherichia coli*: The Role of DnaA in the Control of the SOS Regulon. *Front. Microbiol.* 9. doi: 10.3389/fmicb.2018.01212
- Yavari, N., Goltermann, L., and Nielsen, P. E. (2021). Uptake, stability, and activity of antisense anti-*acpP* PNA-peptide conjugates in *Escherichia coli* and the role of SbmA. *ACS Chem. Biol.* 16, 471–479. doi: 10.1021/acscchembio.0c00822